Electronic Supplementary Material (ESI) for Nanoscale Advances.

Electronic supplementary information: Nanowires exfoliated from one-dimensional van der Waals transition metal trihalides and quadrihalides

Chuanxun Su*,†,‡ and Lixin He*,†,‡

†*CAS Key Laboratory of Quantum Information, University of Science and Technology of China, Hefei, Anhui, 230026, People's Republic of China*

‡*Synergetic Innovation Center of Quantum Information and Quantum Physics, University of Science and Technology of China, Hefei, 230026, People's Republic of China*

E-mail: sucx@ustc.edu.cn; helx@ustc.edu.cn

Structure prototype analysis package

The Structure Prototype Analysis Package (SPAP)[1] is a tool for analyzing the symmetry and similarity of different atomic structures. It is capable of clustering large amounts of atomic structures based on physical features such as symmetry, composition type, and structural distance. SPAP enables the identification of structures in a database that are similar to a target structure. This open-source package is available at: https://github.com/chuanxun/StructurePrototypeAnalysisPackage.

The procedure for querying similar structures in the database involves four steps: (1) selecting structures with the target composition type; (2) adjusting the atom number density of the selected structures to match that of the target structure; (3) calculating the CCFs of the structures and evaluating the distances between the CCFs of the target structure and the

selected structures; (4) ranking the structures in ascending order based on their structural distances. In step 2, we can construct an atom number density normalization coefficient

$$c_{\mathrm{bulk}} = \sqrt[3]{\frac{N_{\mathrm{s}}}{V_{\mathrm{s}}\rho_{\mathrm{t}}}}, \tag{S1}$$

where N_{s}, V_{s}, and ρ_{t} denote the total number of atoms for the selected structure, the volume of the selected structure, and the atom number density of the target structure, respectively. We multiply the 3 lattice vectors of the selected structure by c_{bulk} and the fractional coordinates of the atoms of the selected structure should be kept unchanged. A comparison between structures then reduces to a comparison of the respective $\mathrm{ccf}_{ij}(r)$. We utilize the Pearson correlation coefficient to measure the degree of similarity between $\mathrm{ccf}_{ij}^{A}(r)$ and $\mathrm{ccf}_{ij}^{B}(r)$ from structure A and B, respectively. The Pearson correlation coefficient is calculated for discrete points r_k within the range of 0–10 Å and $r_{\mathrm{cut}} = 9$ Å,

$$R_{ij} = \frac{\sum_{r_k}[\mathrm{ccf}_{ij}^{A}(r_k) - \overline{\mathrm{ccf}_{ij}^{A}}][\mathrm{ccf}_{ij}^{B}(r_k) - \overline{\mathrm{ccf}_{ij}^{B}}]}{\sqrt{\sum_{r_k}[\mathrm{ccf}_{ij}^{A}(r_k) - \overline{\mathrm{ccf}_{ij}^{A}}]^2}\sqrt{\sum_{r_k}[\mathrm{ccf}_{ij}^{B}(r_k) - \overline{\mathrm{ccf}_{ij}^{B}}]^2}}, \tag{S2}$$

where $\overline{\mathrm{ccf}_{ij}^{A}}$ and $\overline{\mathrm{ccf}_{ij}^{B}}$ represent the average values of $\mathrm{ccf}_{ij}^{A}(r_k)$ and $\mathrm{ccf}_{ij}^{B}(r_k)$, respectively. However, Eq. S2 is problematic if $\mathrm{ccf}_{ij}^{A}(r)$ or $\mathrm{ccf}_{ij}^{B}(r)$ equals a constant. From the definition of the CCF we can see that if $\mathrm{ccf}_{ij}(r) = C$, then $\mathrm{ccf}_{ij}(r) = 0$. If a structure has many different types of elements or r_{cut} is small, it is possible that $\mathrm{ccf}_{ij}(r) = 0$ occurs. Table S1 shows how we evaluate R_{ij} for such cases. The distance between $\mathrm{ccf}_{ij}^{A}(r)$ and $\mathrm{ccf}_{ij}^{B}(r)$ can be defined as $d_{ij} = 1 - R_{ij}$. It can be deduced from the definition of CCF that

$$\mathrm{ccf}_{ij}(r) = \mathrm{ccf}_{ji}(r). \tag{S3}$$

Only $\mathrm{ccf}_{ij}(r)$ with $i \leq j$ needs to be calculated and $d_{ij} = d_{ji}$. The summation of d_{ij} with their respective weight factors yields the distance between structures A and B.

Table S1: Evaluation of R_{ij} when $\mathrm{ccf}_{ij}^{A}(r) = 0$ or $\mathrm{ccf}_{ij}^{B}(r) = 0$.

$\sum_{r_k}[\mathrm{ccf}_{ij}^{A}(r_k) - \overline{\mathrm{ccf}_{ij}^{A}}]^2$	$\sum_{r_k}[\mathrm{ccf}_{ij}^{B}(r_k) - \overline{\mathrm{ccf}_{ij}^{B}}]^2$	R_{ij}
0	0	1
0	Non-zero	0
Non-zero	0	0

Total energies for different magnetic configurations

Table S2 shows the total energies of the structures under different magnetic configurations. Various initial magnetizations are applied to obtain different final magnetic states. However, it should be noted that in some compounds such as TiI_3, the systems converge to non-magnetic (NM) states even though the initial states are magnetic.

Table S2: Final magnetization and converged total energies (E) for different initial magnetic configurations.

Compound	Space group	System	Initial magnetism	Final magnetism	E (eV/atom)
TiI_3	$Pmmn$	Bulk	NM	NM	0.0000
TiI_3	$Pmmn$	Bulk	FM	NM	0.0000
TiI_3	$Pmmn$	Bulk	AFM	NM	0.0000
TiI_3		1-chain	NM	NM	0.1643
TiI_3		1-chain	FM	NM	0.1643
TiI_3		1-chain	AFM	NM	0.1643
TiI_3		3-chain	NM	NM	0.1114
TiI_3		3-chain	FM	NM	0.1113
TiI_3		7-chain	NM	NM	0.0725
β-$TiCl_3$	$Pmmn$	Bulk	NM	NM	0.0000
β-$TiCl_3$	$Pmmn$	Bulk	FM	NM	0.0000
β-$TiCl_3$	$Pmmn$	Bulk	AFM	NM	0.0000
$TiCl_3$		1-chain	NM	NM	0.1152
$TiCl_3$		1-chain	FM	NM	0.1152
$TiCl_3$		1-chain	AFM	NM	0.1152
$TiCl_3$		monolayer	NM	NM	0.0792
$TiCl_3$		monolayer	FM	NM	0.0792
$MoBr_3$	$Pmmn$	Bulk	AFM	AFM	0.0000
$MoBr_3$	$Pmmn$	Bulk	FM	FM	0.0170
$MoBr_3$		1-chain	AFM	AFM	0.1358
$MoBr_3$		1-chain	FM	FM	0.1524
β-$RuCl_3$	$Pmmn$	Bulk	NM	NM	0.0000
β-$RuCl_3$	$Pmmn$	Bulk	FM	NM	-0.0002

Continued on next page

Continued

Compound	Space group	System	Initial magnetism	Final magnetism	E (eV/atom)
β-$RuCl_3$	$Pmmn$	Bulk	AFM	NM	0.0000
$RuCl_3$		1-chain	NM	NM	0.1153
$RuCl_3$		1-chain	FM	NM	0.1153
$RuCl_3$		1-chain	AFM	NM	0.1153
$RuBr_3$	$Pmmn$	Bulk	NM	NM	0.0000
$RuBr_3$	$Pmmn$	Bulk	FM	NM	-0.0001
$RuBr_3$	$Pmmn$	Bulk	AFM	NM	0.0000
$RuBr_3$		1-chain	NM	NM	0.1342
$RuBr_3$		1-chain	FM	NM	0.1342
ZrI_3	$Pmmn$	Bulk	NM	NM	0.0000
ZrI_3	$Pmmn$	Bulk	FM	NM	0.0000
ZrI_3	$Pmmn$	Bulk	AFM	NM	0.0000
ZrI_3		1-chain	NM	NM	0.1636
ZrI_3		1-chain	FM	NM	0.1636
ZrI_3		1-chain	AFM	NM	0.1636
CrI_3	$P6_3/mcm$	Bulk	FM	FM	0.0000
CrI_3	$P6_3/mcm$	Bulk	AFM	AFM	0.0007
CrI_3		1-chain	AFM	AFM	0.1558
CrI_3		1-chain	FM	FM	0.1560
CrI_3		3-chain	FM	FM	0.1068
CrI_3		3-chain	AFM	AFM	0.1069
CrI_3		7-chain	FM	FM	0.0697
CrI_3		7-chain	AFM	AFM	0.0699
$TcBr_3$	$Pmmn$	Bulk	FM	FM	0.0000
$TcBr_3$	$Pmmn$	Bulk	AFM	FM	0.0000
$TcBr_3$		1-chain	FM	FM	0.1421
$TcBr_3$		1-chain	AFM	FM	0.1421
$TcBr_4$	$Pbca$	Bulk	AFM	AFM	0.0000
$TcBr_4$	$Pbca$	Bulk	FM	FM	0.0077
$TcBr_4$		1-chain	AFM	AFM	0.1394
$TcBr_4$		1-chain	FM	FM	0.1433

Structure prediction for CrI_3

We use the big data method (BDM)[1] to search for stable bulk structures in the CrI_3 system. Specifically, the BDM selects out AB_3 structure prototypes from the crystal structure prototype database and substitutes the original element types A and B with Cr and I, re-

spectively. The primitive structures are generated with 1 to 8 formula units and their atom number density is adjusted to 0.02703 atom/Å^3. We require that the Cr-Cr, Cr-I, and I-I distances need to be larger than 1.696 Å. Structures that do not meet the minimum interatomic distance requirement are discarded. After screening, 214 structures are successfully generated and we relax all the structures via first-principles calculations. The structures are sorted in ascending order according to their lattice energy per atom.

Electronic band structure and density of states

The electronic band structures and total density of states for 1-chain, 3-chain, and 7-chain TiI_3 NWs are shown in Fig. S1, S2, and S3, respectively. All the TiI_3 NWs are semiconductors. The thicker NW has a smaller band gap compared to the thinner NW.

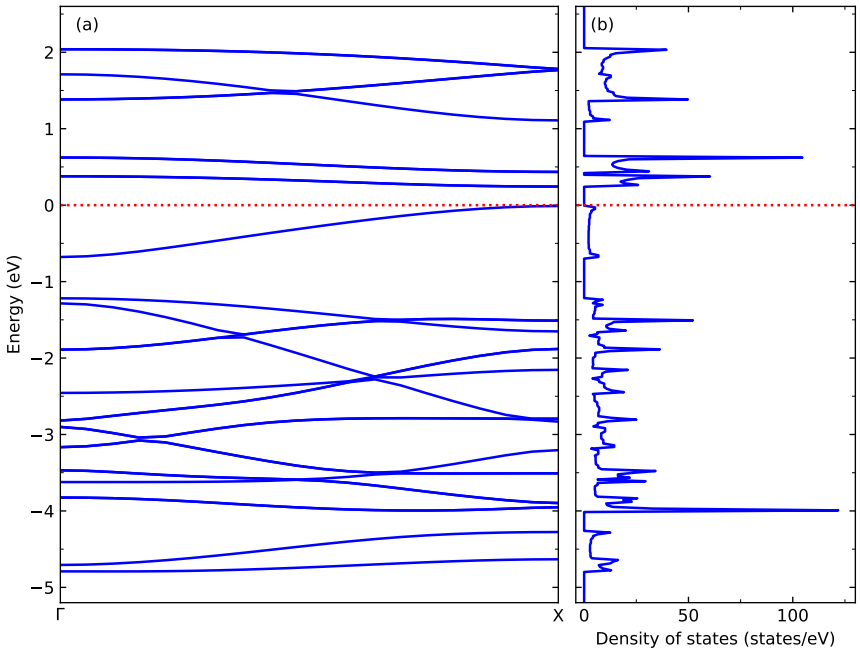

Figure S1: The electronic band structure (a) and total density of states (b) for the 1-chain TiI_3 NW. The dashed line denotes the Fermi level.

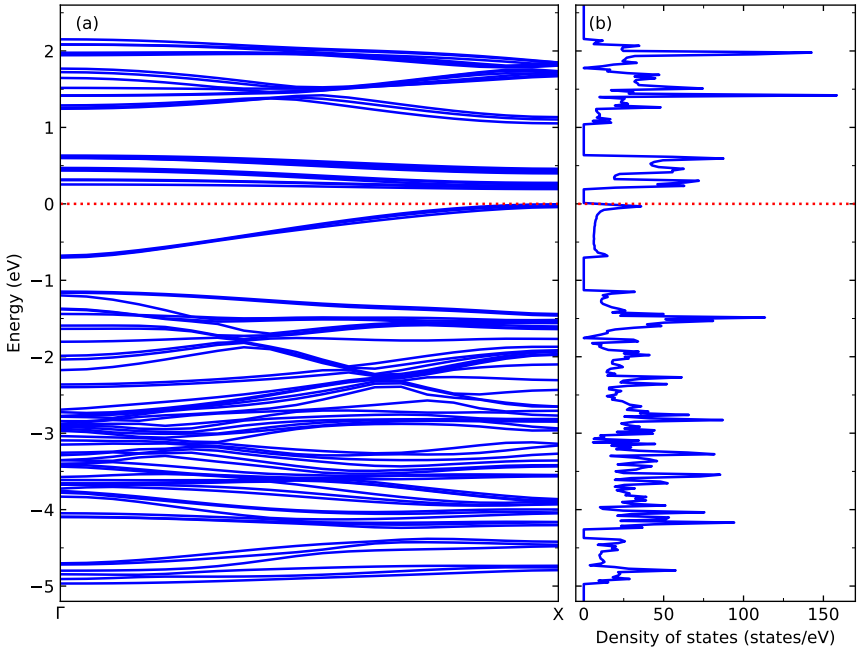

Figure S2: The electronic band structure (a) and total density of states (b) for the 3-chain TiI_3 NW. The dashed line denotes the Fermi level.

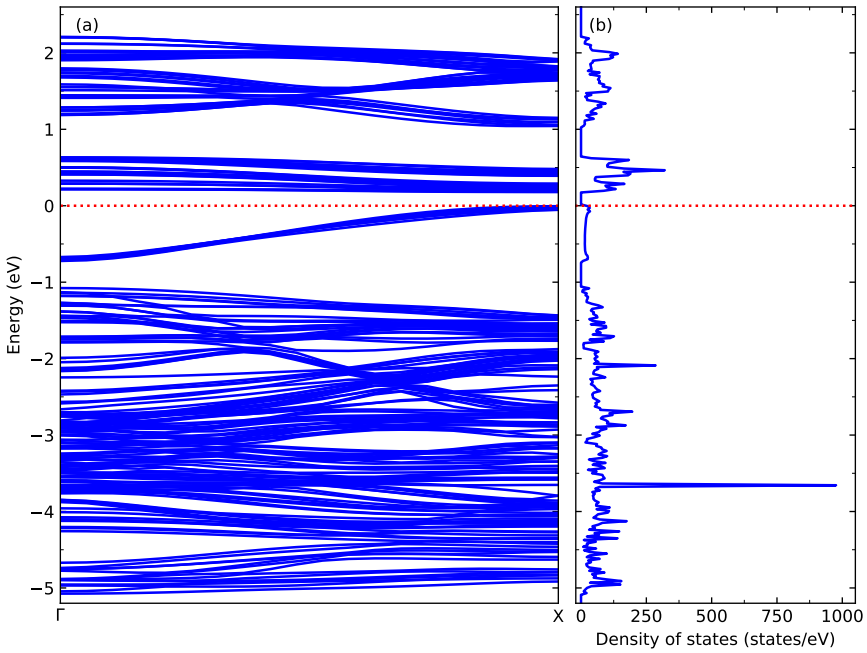

Figure S3: The electronic band structure (a) and total density of states (b) for the 7-chain TiI_3 NW. The dashed line denotes the Fermi level.

Phonon spectra

The phonon spectra are calculated using a supercell approach. Figure S4 shows the phonon spectra of bulk $P6_3/mcm$ CrI_3. The absence of imaginary phonon frequencies indicates that bulk CrI_3 is dynamically stable. Figure S5 shows the phonon spectra of the 1-chain TiI_3, $MoBr_3$, and $RuCl_3$ NWs, and the 3-chain TiI_3 and CrI_3 NWs, and 7-chain TiI_3 NW. These NWs have no or negligible imaginary phonon frequencies, suggesting that they are dynamically stable. Figure S6 displays the phonon spectra of 1-chain $RuBr_3$ and ZrI_3 NWs, which exhibit small imaginary phonon frequencies, indicating that they are dynamically unstable.

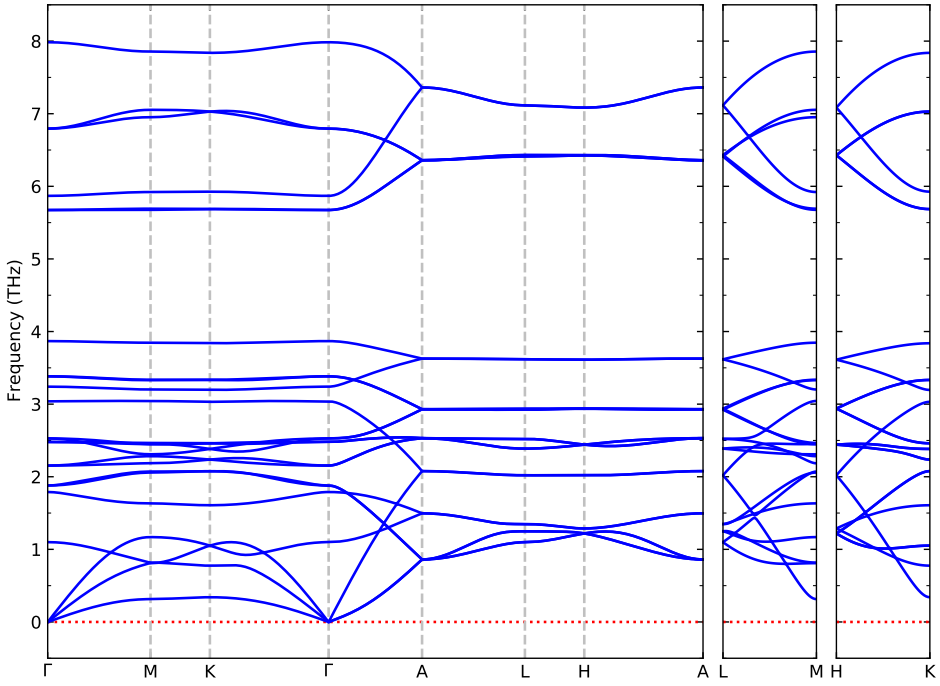

Figure S4: Phonon spectra of bulk $P6_3/mcm$ CrI_3.

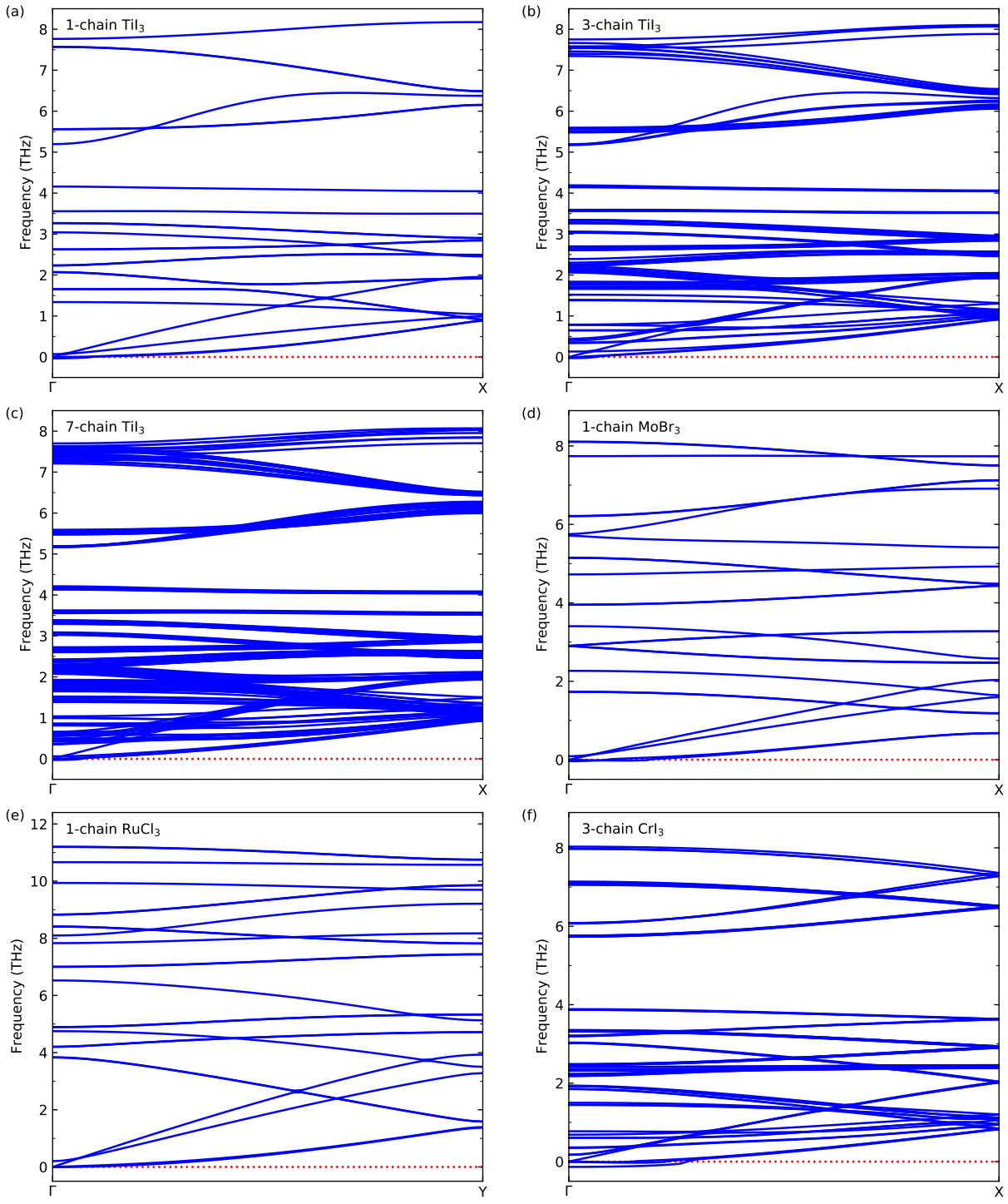

Figure S5: Phonon spectra of the 1-chain TiI_3 (a), 3-chain TiI_3 (b), 7-chain TiI_3 (c), 1-chain $MoBr_3$ (d), 1-chain $RuCl_3$ (e), 3-chain CrI_3 (f).

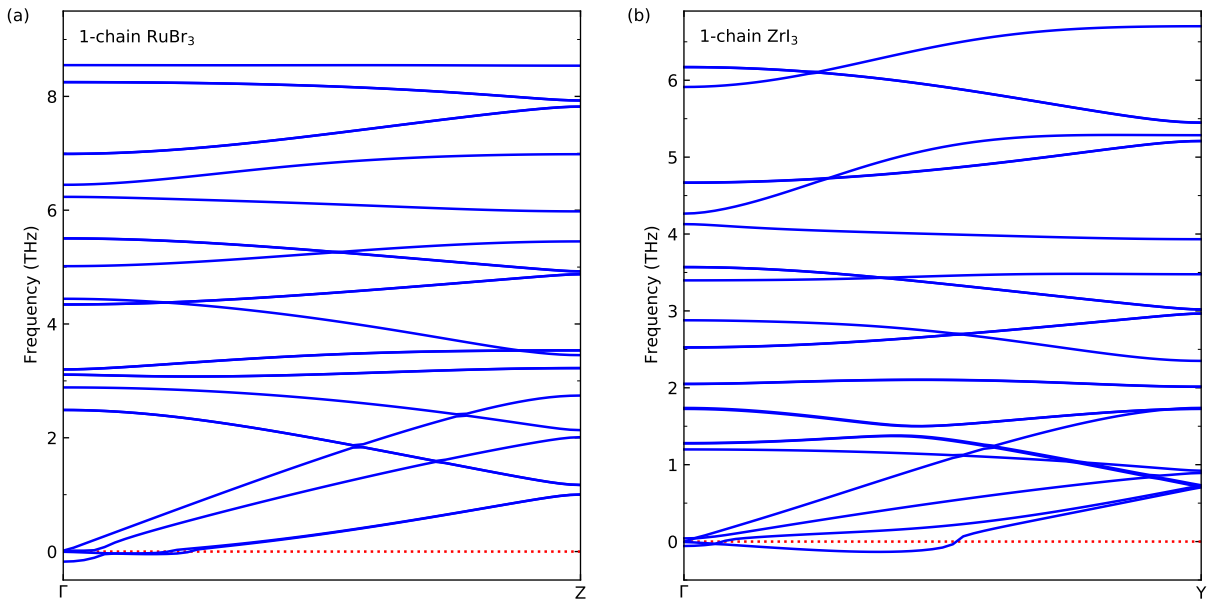

Figure S6: Phonon spectra of the 1-chain $RuBr_3$ (a) and 1-chain ZrI_3 (b).

ab initio molecular dynamics simulations

Ab initio molecular dynamics (AIMD) simulations are performed using supercells, which are extended 4 times the unit cell along the atomic chain, at 300 K for 10 ps. Figure S7 shows the CCFs for the relaxed (static) 1-chain $RuBr_3$ NW and the averaged CCFs for the AIMD simulated 1-chain $RuBr_3$ NWs. Figure S8 shows the CCFs for the relaxed 1-chain $TcBr_3$ NW and the averaged CCFs for the AIMD simulated 1-chain $TcBr_3$ NWs. The $ccf_{ij}^{AIMD}(r)$ at 300 K still maintains the well organized periodicity, suggesting that the 1-chain $RuBr_3$ and $TcBr_3$ NWs preserve the crystal structure, even though their phonon spectra have small soft modes near the Γ point.

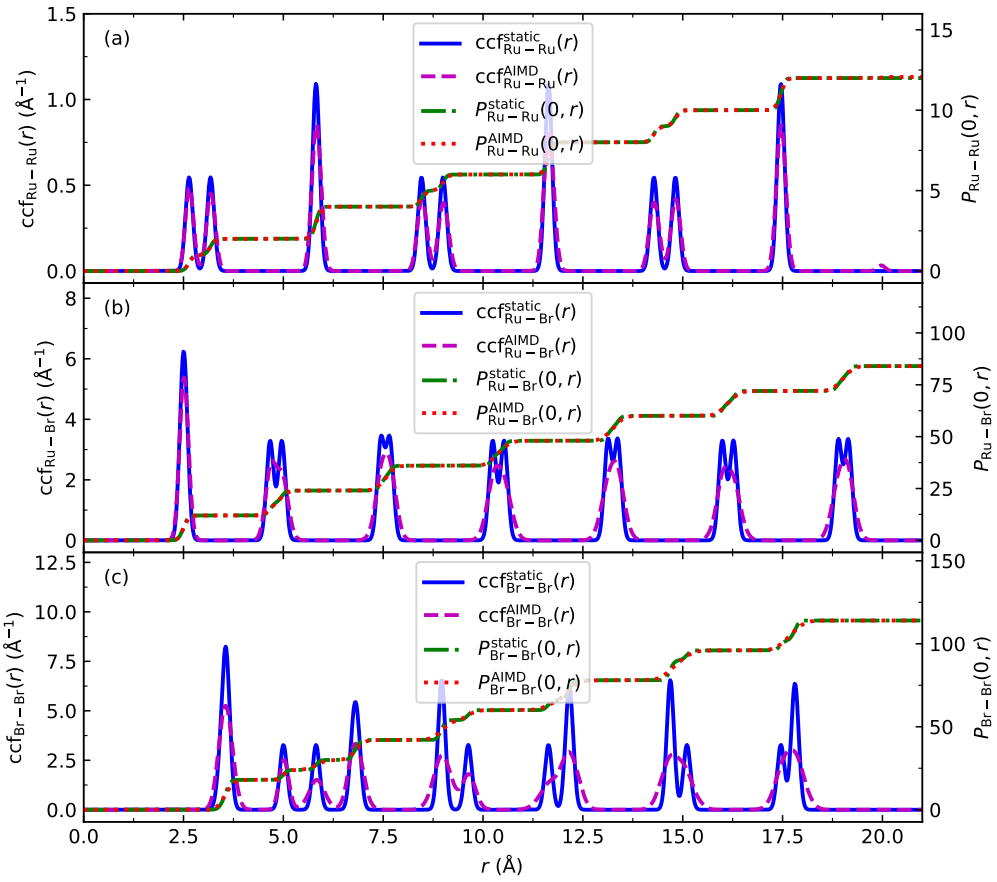

Figure S7: The CCFs for the relaxed 1-chain $RuBr_3$ NW and the averaged CCFs for the AIMD simulated 1-chain $RuBr_3$ NWs at 300 K in the range of (0.5, 10.0) ps, which are denoted by $\mathrm{ccf}_{ij}^{\mathrm{static}}(r)$ and $\mathrm{ccf}_{ij}^{\mathrm{AIMD}}(r)$, respectively. The corresponding pair functions $P_{ij}^{\mathrm{static}}(0,r)$ and $P_{ij}^{\mathrm{AIMD}}(0,r)$ are also shown.

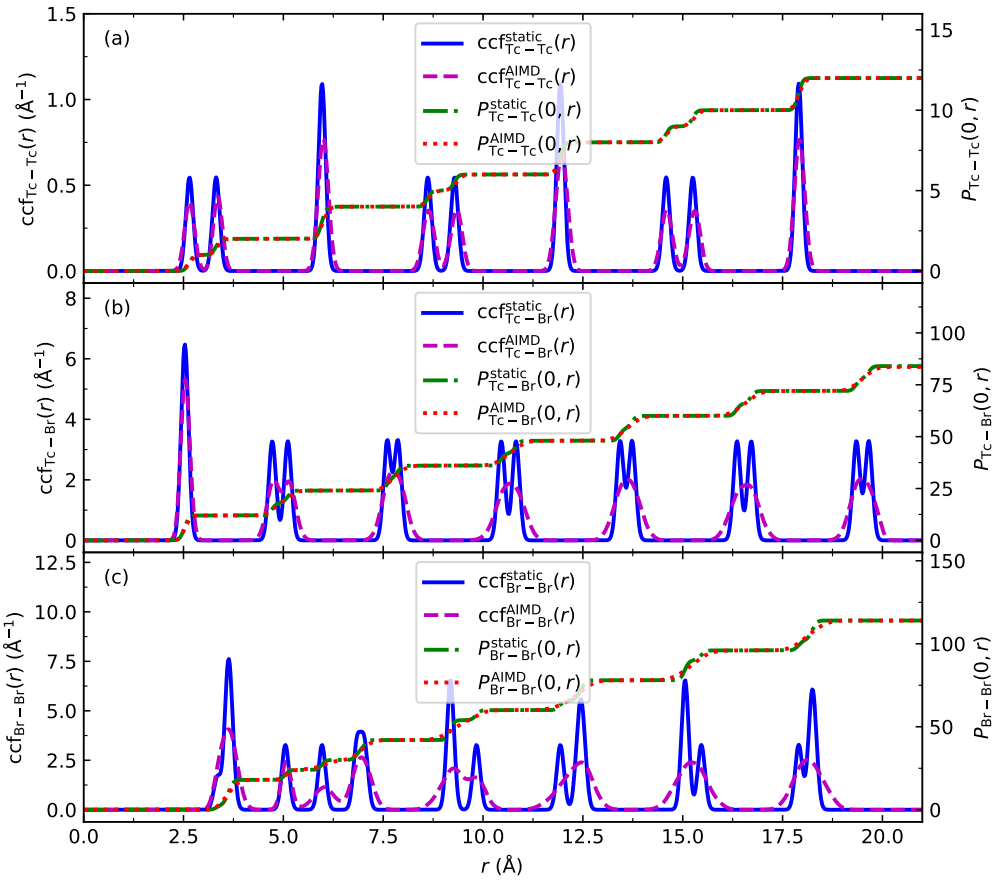

Figure S8: The CCFs for the relaxed 1-chain $TcBr_3$ NW and the averaged CCFs for the AIMD simulated 1-chain $TcBr_3$ NWs at 300 K in the range of (0.5, 10.0) ps, which are denoted by $\mathrm{ccf}^{\mathrm{static}}_{ij}(r)$ and $\mathrm{ccf}^{\mathrm{AIMD}}_{ij}(r)$, respectively. The corresponding pair functions $P^{\mathrm{static}}_{ij}(0,r)$ and $P^{\mathrm{AIMD}}_{ij}(0,r)$ are also shown.

References

(1) Su, C.; Lv, J.; Li, Q.; Wang, H.; Zhang, L.; Wang, Y.; Ma, Y. Construction of crystal structure prototype database: methods and applications. *J. Phys.: Condens. Matter* **2017**, *29*, 165901–165901.